Original Article

REGγ deficiency ameliorates hepatic ischemia and reperfusion injury in a mitochondrial p66shc dependent manner in mice

Long Guo[#^], Qing Yang[#], Jiali Zhu, Jinbao Li

Department of Anesthesiology, Shanghai General Hospital, Shanghai Jiao Tong University School of Medicine, Shanghai, China

Contributions: (I) Conception and design: J Li, J Zhu; (II) Administrative support: J Li, J Zhu; (III) Provision of study materials or patients: J Li, J Zhu; (IV) Collection and assembly of data: L Guo, Q Yang; (V) Data analysis and interpretation: L Guo, Q Yang; (VI) Manuscript writing: All authors; (VII) Final approval of manuscript: All authors.

[#]These authors contributed equally to this work.

Correspondence to: Jinbao Li, MD; Jiali Zhu, MD. Department of Anesthesiology, Shanghai General Hospital, Shanghai Jiao Tong University School of Medicine, 100 Haining Road, Shanghai 200080, China. Email: lijinbaoshanghai@163.com; jialihappy@163.com.

Background: Hepatic ischemia and reperfusion (I/R) injury is a common problem faced by patients undergoing clinical liver transplantation and hepatectomy, but the specific mechanism of liver I/R injury has not been fully elucidated. The protein degradation complex 11S proteasome is involved in apoptosis, proliferation and cell cycle regulation by regulating the 11S proteasome regulatory complex (REG)γ. The main objective of this study is to explore the role and specific mechanism of REGγ in liver I/R.

Methods: By constructing a model of *in vivo* hepatic I/R injury in mice and a model of hypoxia and reoxygenation (H/R) in isolated hepatocytes. First, the REGγ expression were detected during hepatic I/R in mice. Second, to investigate the effects of REGγ knockout (KO) on liver necrosis, inflammatory response, apoptosis and mitochondrial function. Finally, mouse liver Src homology collagen (p66shc) mitochondrial translocation was detected.

Results: The expression of REGγ was up-regulated during hepatic I/R. REGγ KO had significantly reduced liver tissue infarct size, liver transaminases, inflammatory cells infiltration, inflammatory cytokine and activation of nuclear factor kappa-B (NF-κB) signaling pathway and cell apoptosis. REGγ KO had significantly alleviated the mitochondrial damage, decreased the up-regulated level of cytochrome C, reactive oxygen species (ROS). REGγ KO had significantly reduced p66shc mitochondrial translocation in mice.

Conclusions: The experimental results of this study indicated that REGγ has an important role in preventing liver I/R injury and may play a role through the mitochondrial p66shc signaling pathway.

Keywords: Ischemia and reperfusion (I/R); the 11S proteasome regulatory complex γ (REGγ); p66shc; mitochondrial function; apoptosis

Received: 11 April 2024; Accepted: 31 July 2024; Published online: 16 October 2024.

doi: 10.21037/tgh-24-46

View this article at: https://dx.doi.org/10.21037/tgh-24-46

Introduction

Hepatic ischemia and reperfusion (I/R) injury is one of the major complications of hemorrhagic shock and liver surgery, including hepatic tumor resection and liver transplantation (1,2). Alleviating liver I/R damage may improve the prognosis of patients in clinical settings, while the specific mechanisms of hepatic I/R injury have not been fully elucidated (3).

Hepatic I/R injury is a biphasic phenomenon in which cellular damage caused by the interruption of blood supply to tissues during ischemia (4). The blood supply was

^ ORCID: 0000-0002-7756-9348.

restored after reperfusion and cells switched to aerobic metabolism, resulted in severe oxidative stress. Hepatocyte injury or death was I due to energy deprivation, aseptic inflammation, oxidative stress, and other factors (5,6). Guo *et al.* had focused on studying the regulatory mechanisms of hepatic I/R injury, including Kupffer cells and neutrophils activation and apoptosis due to mitochondrial damage, and it has been demonstrated that it was possible to improve hepatic I/R injury by interventions such as reducing inflammation (7).

The proteasome is an important way for regulating protein stability In eukaryotes (8), which comprises a 20S core subunit and two regulatory units. The 11S proteasome regulatory complex (REG) binds to 20S to form the REG-20S-REG complex (9,10). The REG family comprises REGα, REGβ, and REGγ. REGα and REGβ are primarily expressed in the cytoplasm, whereas REGγ is mostly found in the nucleus, although it has been reported to play a significant role in the cytoplasm (11).

REGγ, also known by other names like PA28γ, Ki antigen, or PSME3, performing various physiological and pathological regulatory functions through the degradation of specific target proteins like SRC-3 (12), p21 (13), CK1δ (14), iκBε (15), GSK3β (16), and playing a part in inflammatory diseases such as testicular inflammation (17), inflammatory bowel disease (18), systemic lupus erythematosus (19), and others. Moreover, a recent research paper discovered that REGγ knockdown significantly suppressed liver tumor formation by regulating mTORC1 and glycolysis during the development of hepatocellular carcinoma (20), suggesting that REGγ may play a significant role in liver diseases. Nonetheless, the exact part played by REGγ in the hepatic I/R process has not yet been reported.

Highlight box

Key findings

- The 11S proteasome regulatory complex (REG)γ has an important role in preventing liver ischemia and reperfusion (I/R) injury.

What is known and what is new?

- REGγ is involved in apoptosis, proliferation and cell cycle regulation.
- REGγ knockout (KO) reduces hepatic I/R injury by reducing inflammatory response and mitochondrial damage.

What is the implication, and what should change now?

- REGγ KO prevents hepatic I/R injury and may exert its effect through the mitochondrial p66shc signaling pathway.

We present this article in accordance with the ARRIVE reporting checklist (available at https://tgh.amegroups.com/article/view/10.21037/tgh-24-46/rc).

Methods

Animals

We maintained REGγ$^{+/-}$ mice (C57BL/6 genetic background) intercrossed for over 10 generations to acquire REGγ$^{-/-}$ mice. C57/BL 6 mice (8 weeks old, 23±2 g) were purchased from Jihui Laboratory Animal Care Co., Ltd (Shanghai, China). The mice were housed in a clean room maintained at 24±2 ℃ under a 12 h: 12 h light: dark cycle, with free access to food and water. All experimental animals were approved by Clinical Center Laboratory Animal Welfare & Ethics Committee of Shanghai General Hospital, Shanghai Jiao Tong University (No. 2020AWS0032). All applicable international, national, and/or institutional guidelines for the care and use of animals were followed. A protocol was prepared before the study without registration.

Experimental design

Forty-two mice were completely randomly divided into four groups: (I) two sham group (n=18), in which mice underwent sham operation and received saline; (II) two I/R group (n=24), in which mice were subjected to hepatic I/R and received saline.

Hepatic I/R model

As described, we used an established partial 75% liver warm I/R model (21). In brief, Firstly, anesthetize the mice, and then use microvascular clamping to supply blood to the portal vein and hepatic artery in the left and middle lobes of the liver. After 60 minutes of partial liver ischemia, remove the clamp to start different reperfusion time points.

Isolation of primary hepatocytes

As mentioned earlier (21,22), primary liver cells were isolated from the liver and cells with a survival rate higher than 90% were used for further experiments.

Hypoxia and reoxygenation (H/R) model

To simulate *in vivo* I/R models and explore the underlying

molecular mechanisms, we constructed an *in vitro* H/R model of liver cells. The liver cells were incubated in a pH 6.2 culture medium in an anaerobic chamber for 4 hours. To simulate the physiological pH of reperfusion, the anaerobic Krebs-Ringer-HEPES (KRH) at pH 6.2 was replaced with aerobic KRH at pH 7.4, and the cells were incubated in different aerobic environments. The corresponding processing was performed after the interval. this model was similar to those reported before (23).

Histopathology

The collected liver tissues were soaked in 4% paraformaldehyde for 48 h and then embedded in paraffin. Liver sections were stained with Hematoxylin-eosin staining (H&E). The severity of liver I/R tissue damage was assessed according to percentage of necrotic area.

Aminotransferase assessment

As indices of hepatocellular injury, the serum and liver tissue levels of alanine aminotransferase (ALT) and aspartate aminotransferase (AST) were measured with ALT and AST microplate test kit. The ALT and AST microplate test kits (Jiancheng Biotech, C009-2-1, China).

Western blot (WB)

Samples were lysed using RIPA lysis buffer. Significant amounts of proteins (50–60 μg) were separated by Lamide gel electrophoresis. Polyvinylidene difluoride (PVDF) protein transfer membranes were immobilized with 3%/5% skim milk or BSA for 2 hours. The membranes were then incubated with specific primary antibodies overnight at 4 ℃ and with HRP-conjugated secondary antibodies for 2 hours at RT. Finally, the PVDF membranes were washed with PBS for 1 hour. Immunoreactive bands were visualized using the BIORAD ChemiDoc XRS system, and densitometric analysis was performed using Image J software. Primary antibodies as following: 78–82 Kda hosphor-DRP1 Rabbit 1:1000, CST (Shanghai, China); 83 Kda DRP1 Rabbit 1:1000, Abcam (Shanghai, China); 61/55 Kda hosphor-NF-κB p65 Rabbit 1:1000, Bioss (Beijing, China); 65 Kda NF-κB p65 Rabbit 1:2000, Bioss; 36 Kda p-IκBα Rabbit 1:2000, CST; 36 Kda IκBα Rabbit 1:2000, CST; 35 Kda Caspase-3 Rabbit 1:1000, CST; 17/19 Kda Cleaved Caspase-3 Rabbit 1:1000, CST; 21 Kda BCL2-associated X protein (BAX) Rabbit 1:1000, Proteintech (Wuhan, China); 26 Kda B-cell lymphoma-2 (BCL-2) Rabbit 1:1000, Proteintech; 42 Kda β-actin Mouse 1:5000, Proteintech; 63/67–75 Kda p66shc Rabbit 1:1000, Proteintech; 63/55 Kda p-ser36 p66shc Mouse 1:1000, Abcam; 36 Kda GAPDH Rabbit 1:5000, Affinity (Nanjing, China); 12–15 Kda Cytochrome C Mouse 1:5000, Proteintech; 17–18 Kda COXIV Rabbit 1:5000, Proteintech; 35 REGγ Rabbit 1:2000, Proteintech.

Liver tissue immunofluorescence

Immunohistochemical staining was performed using specific antibodies against Ly-6G (Servicebio, GB11229, Wuhan, China), F4/80 (Servicebio, GB11027), cleaved caspase-3 (CST, Asp175). Incubation with the respective primary antibody was carried out at 4 ℃ for 2 h, followed by sealing with an anti-fluorescence quenching mounting medium containing DAPI. Micrographs of liver slices were captured using a Leica DMi8 microscope, and fluorescence analysis was conducted using Image J software.

Flow cytometry (FCM)

The infiltration of neutrophils and macrophages in the liver of mice was determined by FCM. Fluorescence binding PE-anti-Ly-6G (eBioscience, 12-5931-81, San Diego, CA, USA) were used to label neutrophils, FITC-anti-F4/80 (BioLegend, 123127, San Diego, CA, USA) antibodies were used to label macrophages.

Quantitative real-time polymerase chain reaction (qRT-PCR)

Following the extraction of RNA from the liver using Trizol, cDNA was generated by reverse transcription of RNA (1 μg) using the 2x S6 Universal SYBR qPCR Mix (#Q204-02, EnzyArtisan). The following primer sequence was used for reverse transcription of cDNA into complementary DNA: IL-1β, 5'-GAAATGCCACCTTTTGACAGTG-3' and 5'-TGGATGCTCTCATCAGGACAG-3';

TNF-α, 5'-CAGGCGGTGCCTATGTCTC-3' and 5'-CGATCACCCCGAAGTTCAGTAG-3';

IL-6, 5'-CTGCAAGAGACTTCCATCCAG-3' and 5'-AGTGGTATAGACAGGTCTGTTGG-3';

18S, 5'-TTCCGATAACGAACGAGACTCT-3' and

5'-TGGCTGAACGCCACTTGTC-3'.

Terminal deoxynucleotidyl transferase mediated dUTP nick-end labeling (TUNEL)

TUNEL kit (Servicebio, G1504) was used to detect liver apoptosis. In short, use this technique to stain paraffin embedded liver tissue sections. tissue sections were cultured in TUNEL reaction mixture. Then, it was stained with 4',6-diamino-2-phenylindole (DAPI). The apoptotic index TUNEL positive cell number/total liver cell number was calculated for each mouse.

Observation of liver mitochondria

The mitochondria of mice liver were detected by Transmission Electron Microscope (TEM). Following a 24 h fixation period with 2.5% glutaraldehyde, fresh mouse livers were treated with 1% osmium tetroxide for one hour and then dehydrated with a graded alcohol series. Subsequently, lead citrate and uranyl acetate were applied to stain the Epon resin embedded particles. The average diameter of mitochondria was used for statistical analysis of mitochondrial division and fusion status.

Mitochondrial membrane potential (JC-1)

The transition from JC-1 aggregates red to JC-1 monomeric green fluorescence indicates a decrease in cell membrane potential. In brief, the mitochondrial membrane potential detection kit (JC-1) was procured from Beyotime Biotechnology Co., Ltd. (C2006, Shanghai, China). The reduction in mitochondrial membrane potential can be quantified by the transition of JC-1 from red to green fluorescence. The probe loading procedure is as follows: The 6 well plate cells that have undergone H/R treatment should be removed and 1ml of JC-1 staining solution added. The cells should then be incubated at 37 ℃ in a cell culture incubator for 20–30 min. Following the incubation period at 37 ℃, and the cells should be washed twice with JC-1 staining buffer (1×). A volume of 2 mL of cell culture solution should then be added, and the cells should be observed under a fluorescence (Lecia, DMi8, Berlin, Germany). and ImageJ software was utilized to quantify the fluorescent intensity.

Reactive oxygen species (ROS) detection

ROS content in hepatic cells was evaluated with a fluorometric ROS kit (Beyotime Biotechnology Co., Ltd. S0033S). In 24-well plates, hepatic cells were seeded and pretreated with the H/R model as depicted, hepatocytes were incubated with 2',7'-dichlorodihydrofluorescein diacetate (DCFH-DA) for 1h in the dark, after which they were washed with PBS. Photomicrographs of cells were captured with the fluorescence microscope (Lecia, DMi8).

Statistical analysis

All data are expressed as the mean ± standard deviation (SD). Statistical analysis was performed using SPSS Statistics version 17.0 Program (SPSS Inc., Chicago, USA). Graphs were plotted by Prism 7.0 (GraphPad Software, San Diego, CA, USA). The differences among the groups were compared by one-way analysis of variance (ANOVA) followed by Tukey's multiple comparison test. $P<0.05$ was considered statistically significant.

Results

REGγ expression is significantly up-regulated during hepatic I/R injury

In order to verify the specific expression of REG family in mouse liver I/R model, the expression of REG family in liver tissue was detected. The results showed that, the expression of REGγ in liver tissue was up-regulated at 6 and 12 h of hepatic I/R, while the expression of REGα and REGβ did not change significantly (*Figure 1A,1B*). The expression of REGγ was assessed via immunohistochemistry and found to be significantly upregulated (*Figure 1C,1D*). To further explore whether the up-regulation of REGγ occurred in hepatocytes, we performed an *in vitro* H/R experiment in hepatocytes. The results demonstrated that consistent with *in vivo* findings (*Figure 1E,1F*).

REGγ$^{-/-}$ alleviates hepatic I/R injury in mice

HE staining was initially performed. Notably, mice in the REGγ$^{-/-}$-I/R group displayed a significantly smaller infarct area compared to WT-I/R group (*Figure 2A,2B*). Secondly, we tested the levels of ALT/AST in serum and liver tissue,

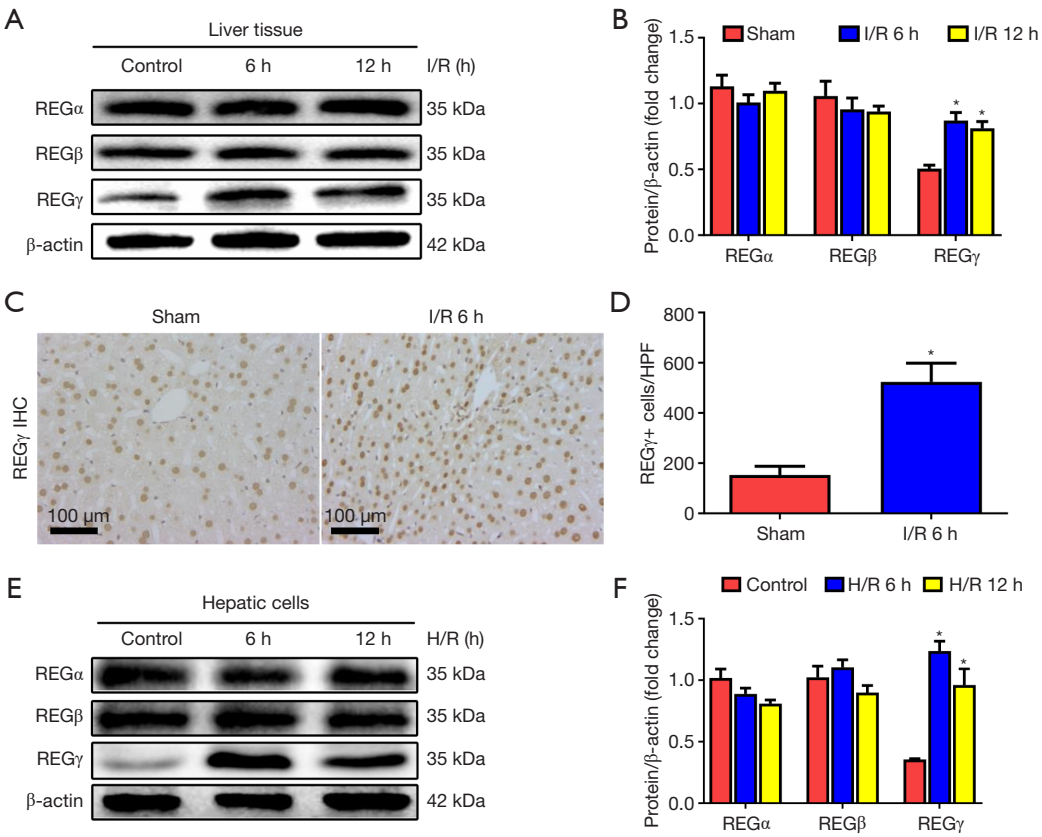

Figure 1 REGγ expression is significantly up-regulated during hepatic I/R injury. WB of REGα, REGβ and REGγ in liver tissue (A), gray value analysis (B), n=3 per group. *, P<0.05 *vs.* control group. Immunohistochemical staining of REGγ in liver tissue (C), scale bar 100 μm, positive cell analysis (D), n=4 per group. *, P<0.05 *vs.* Sham group. *In vitro* experiments: WB of REGα, REGβ and REGγ in hepatocytes (E), gray value analysis (F), n=3 in each group, *, P<0.05 *vs.* control group. I/R, ischemia and reperfusion; REG, the 11S proteasome regulatory complex; WB, Western blot.

the REGγ$^{-/-}$-I/R group exhibited significantly lower levels of transaminases than WT-I/R group (*Figure 2C,2D*).

REGγ$^{-/-}$ alleviates inflammatory response during hepatic I/R injury

To investigate the impact of REGγ on the inflammatory response in hepatic I/R injury, we assessed neutrophils and macrophages infiltration in liver tissue using immunofluorescence and FCM. The results revealed that the REGγ$^{-/-}$-I/R group exhibited significantly reduced neutrophil infiltration in liver tissue when compared to WT-I/R group (*Figure 3A-3D*). And then the infiltration of macrophages in the REGγ$^{-/-}$-I/R group was significantly reduced compared with WT-I/R group (*Figure 3E-3H*).

Additionally, the mRNA expression levels of inflammatory factors (IL-1β, IL-6, TNF-α) in liver tissues were assessed using PCR. The findings revealed that the levels were significantly reduced in the REGγ$^{-/-}$-I/R group compared to WT-sham group (*Figure 3I*).

Finally, WB revealed *in vivo* activation of the NF-κB inflammatory signaling pathway. The results demonstrated that the phosphorylation levels of IκBα and p65 NF-κB were significantly lower in the REGγ$^{-/-}$-I/R group compared to WT-I/R group (*Figure 3J,3K*).

REGγ$^{-/-}$ inhibits cell apoptosis during hepatic I/R injury

In order to explore the effect of REGγ on apoptosis of liver I/R, we first used fluorescent TUNEL staining to detect the changes of apoptosis, and the results showed that the apoptosis of cells in the REGγ$^{-/-}$-I/R group was significantly reduced compared with the WT-I/R group (*Figure 4A,4B*).

Secondly, WB was used to detect the changes of

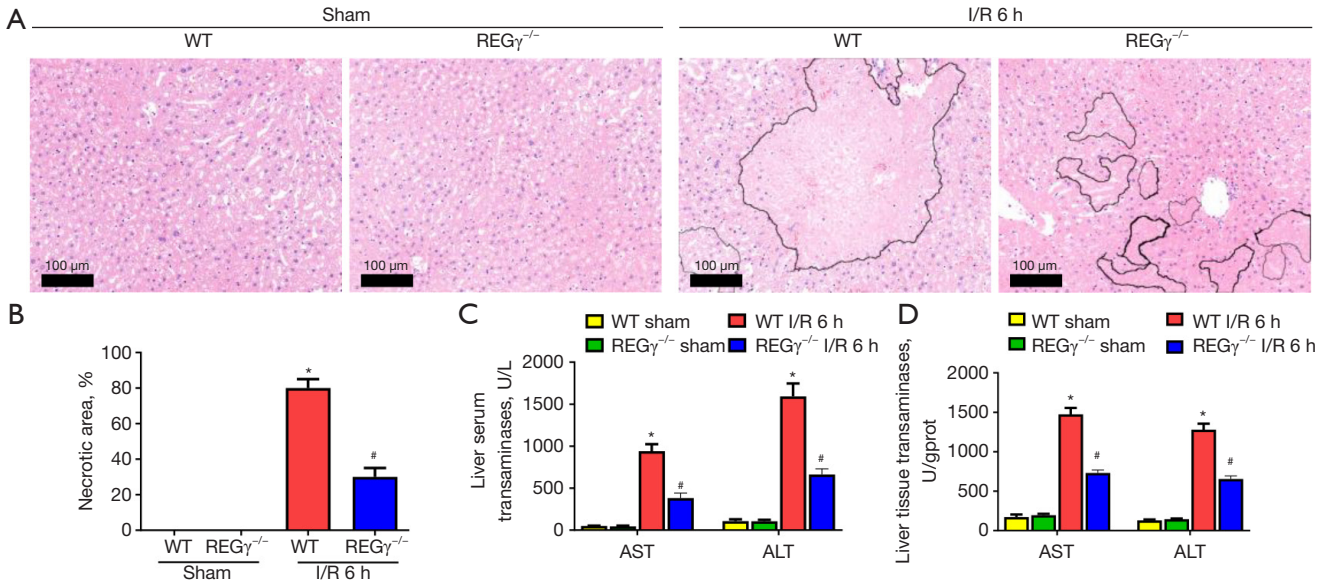

Figure 2 REGγ$^{-/-}$ alleviates hepatic I/R injury in mice. HE staining, scale bar 100 μm (A), damage area analysis (B). AST and ALT level in serum (C), AST and ALT level in liver tissue (D). n=5 per group, *, P<0.05 *vs.* WT-Sham; $^{\#}$, P<0.05 *vs.* WT-I/R group. I/R, ischemia and reperfusion; WT, wild type; REG, the 11S proteasome regulatory complex; HE, hematoxylin-eosin; AST, aspartate aminotransferase; ALT, alanine aminotransferase.

apoptosis-related proteins. The results showed that the levels of anti-apoptotic protein (BCL-2) in the REGγ$^{-/-}$-I/R group were significantly higher than WT-I/R group, while the levels of apoptosis-associated protein (BAX and cleaved caspase3) were significantly lower than WT-I/R group (*Figure 4C,4D*).

Finally, immunofluorescence was used to detect the protein expression of cleaved caspase3, and the results showed that the cleaved caspase3 levels in the REGγ$^{-/-}$-I/R group was significantly lower than WT-I/R group (*Figure 4E,4F*).

REGγ$^{-/-}$ protects hepatocytes from mitochondrial injury during hepatic I/R injury

We first used transmission electron microscopy to analyze mitochondrial morphology, and the results showed that: all hepatocyte mitochondria in the WT-I/R group had obvious structural damage (mitochondrial swelling, ridge disappearance, membrane dissolution, and even vacuolar appearance) and severe mitochondrial division, which was manifested as a significant decrease in mitochondrial diameter. However, mitochondrial damage and division in the REGγ$^{-/-}$-I/R group were significantly reduced compared with WT-I/R group (*Figure 5A,5B*).

Secondly, WB verified the expression of proteins related to mitochondrial division and fusion in the liver I/R, and the results showed that the expression level of phosphorylated DRP1 (Ser637) in REGγ$^{-/-}$-I/R group was significantly higher than WT-I/R group, while the expression level of total protein DRP1 was significantly lower than WT-I/R group (*Figure 5C,5D*).

Subsequently, WB was used to verify the expression of cytochrome C in the liver I/R, and the results showed that the level of cytochrome C in the REGγ$^{-/-}$-I/R group was significantly lower than that in the WT-I/R group (*Figure 5E,5F*).

Finally, fluorescent staining was used to detect the changes of JC-1 and ROS in primary hepatocytes. The results showed that JC-1 aggregates/monomers fluorescence ratio in REGγ$^{-/-}$-H/R group was significantly higher than WT-H/R group (*Figure 5G,5H*). In addition, ROS activation in hepatocytes of REGγ$^{-/-}$-H/R group was significantly decreased compared with WT-H/R group (*Figure 5I,5J*). These results suggest that REGγ$^{-/-}$ can alleviate mitochondrial dysfunction and oxidative stress in mouse liver I/R.

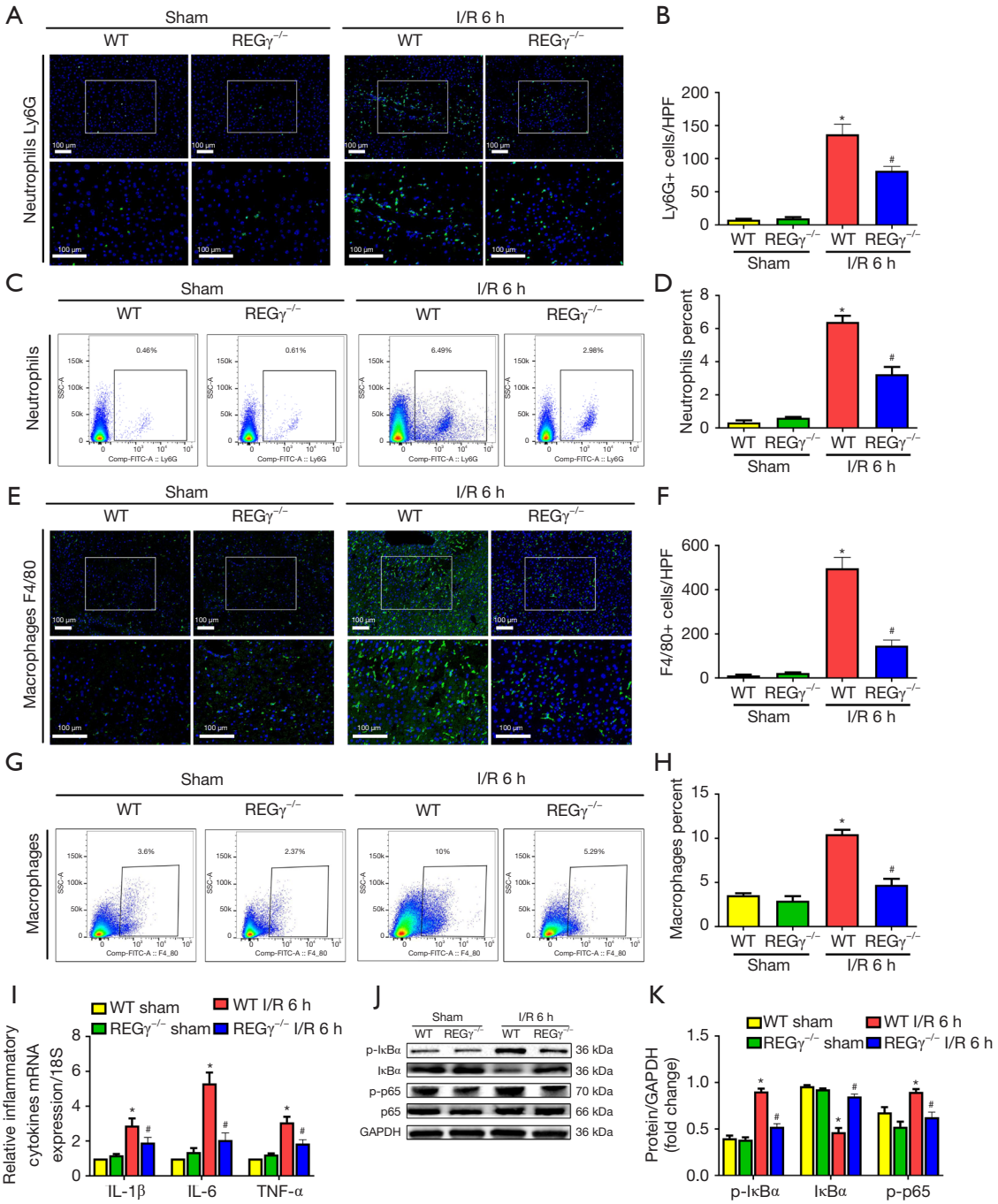

Figure 3 REGγ$^{-/-}$ alleviates hepatic inflammatory response in mice. Neutrophil immunofluorescence staining, scale bar 100 μm; and positive cell ratio analysis (A,B), n=4 per group. Neutrophils flow cytometry and positive cell ratio analysis (C,D), n=4 per group. Macrophages immunofluorescence staining, scale bar 100 μm; and positive cell ratio analysis (E,F), n=4 per group. Macrophages flow cytometry and positive cell ratio analysis (G,H) n=4 per group. The inflammatory factors (IL-1β, IL-6, and TNF-α) mRNA levels (I). n=6 per group. WB of NF-κB signaling pathway (p-IκBα/IκBα, p-p65/p65) and gray value analysis (J,K). n=5 per group, *, P<0.05 *vs.* WT-Sham group, $^{\#}$, P<0.05 *vs.* WT-I/R group. I/R, ischemia and reperfusion; WT, wild type; REG, the 11S proteasome regulatory complex; IL-1β, interleukin-1β; IL-6, interleukin-6; TNF-α, tumor necrosis factor-α; WB, Western blot; NF-κB, nuclear factor kappa-B; p-p65, phosphorylated p65.

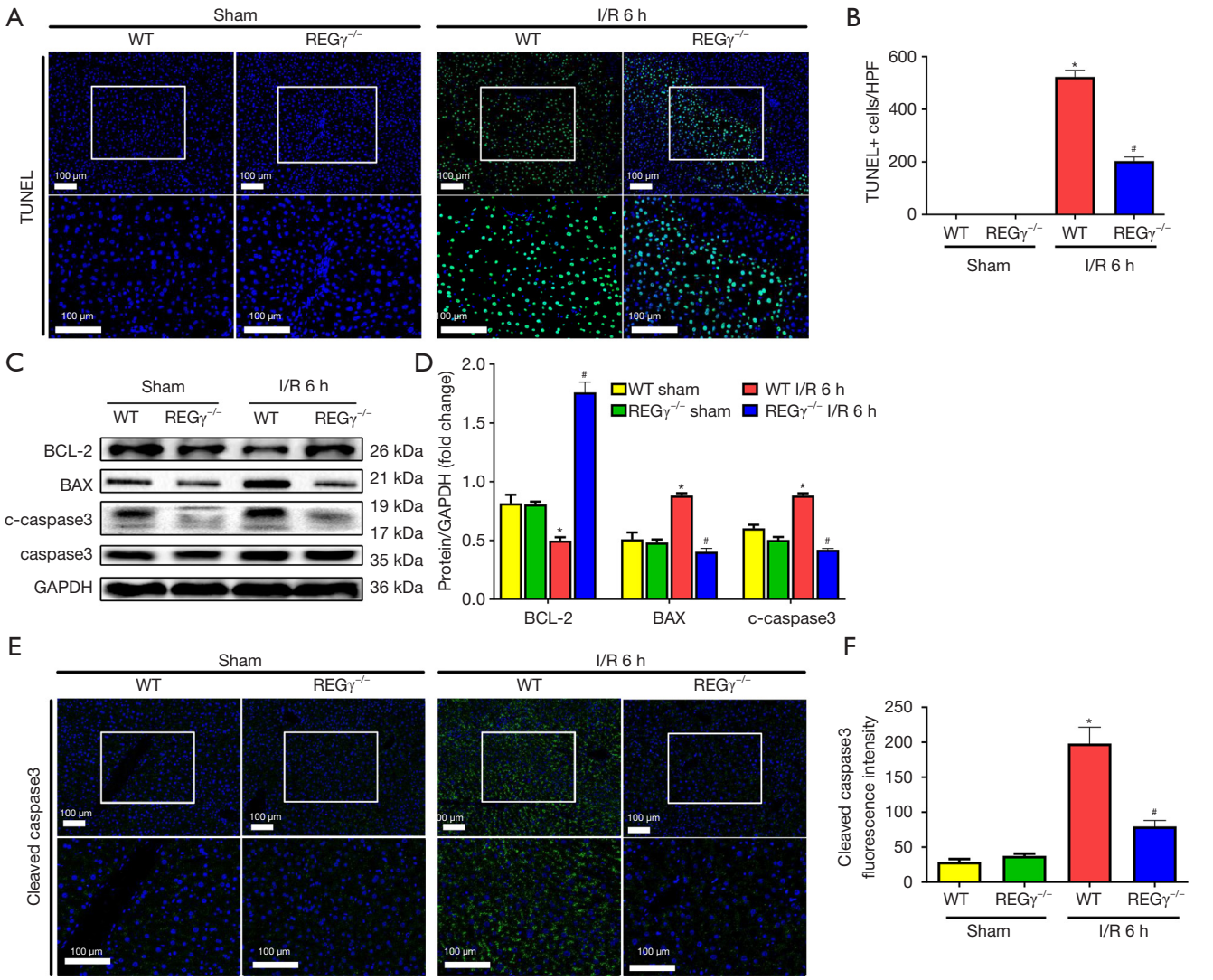

Figure 4 REGγ$^{-/-}$ inhibits hepatic apoptosis in mice. TUNEL immunofluorescence staining, scale bar 100 μm (A), TUNEL-positive cells were analyzed (B). WB of BCL-2, BAX and cleaved caspase3 (C), gray degree value analysis (D). Immunofluorescence staining for cleaved caspase3, scale bar 100 μm (E), mean fluorescence intensity (MFI) analysis of cleaved caspase3 (F). n=5 per group, *, P<0.05 *vs.* WT-Sham, $^{\#}$, P<0.05 *vs.* WT-I/R group. I/R, ischemia and reperfusion; WT, wild type; REG, the 11S proteasome regulatory complex; BCL-2, B-cell lymphoma-2; BAX, BCL2-associated X protein; TUNEL, terminal deoxynucleotidyl transferase mediated dUTP nick-end labeling; WB, Western blot.

REGγ$^{-/-}$ reduces p66shc mitochondrial translocation during hepatic I/R injury

WB of p66shc expression and phosphorylation levels *in vivo* showed that the total protein p66shc and phosphorylation p66shc in the REGγ$^{-/-}$-I/R group were significantly lower than WT-I/R group (*Figure 6A,6B*). In addition, p66shc in mitochondria of the REGγ$^{-/-}$-I/R group was significantly lower than WT-I/R group (*Figure 6C,6D*). These results suggest that REGγ$^{-/-}$ can improve the activation of p66shc and reduce its mitochondrial translocation during hepatic I/R in mice.

Discussion

It has been demonstrated that REGγ KO mice exhibit enhanced autophagy and reduced hepatic steatosis through

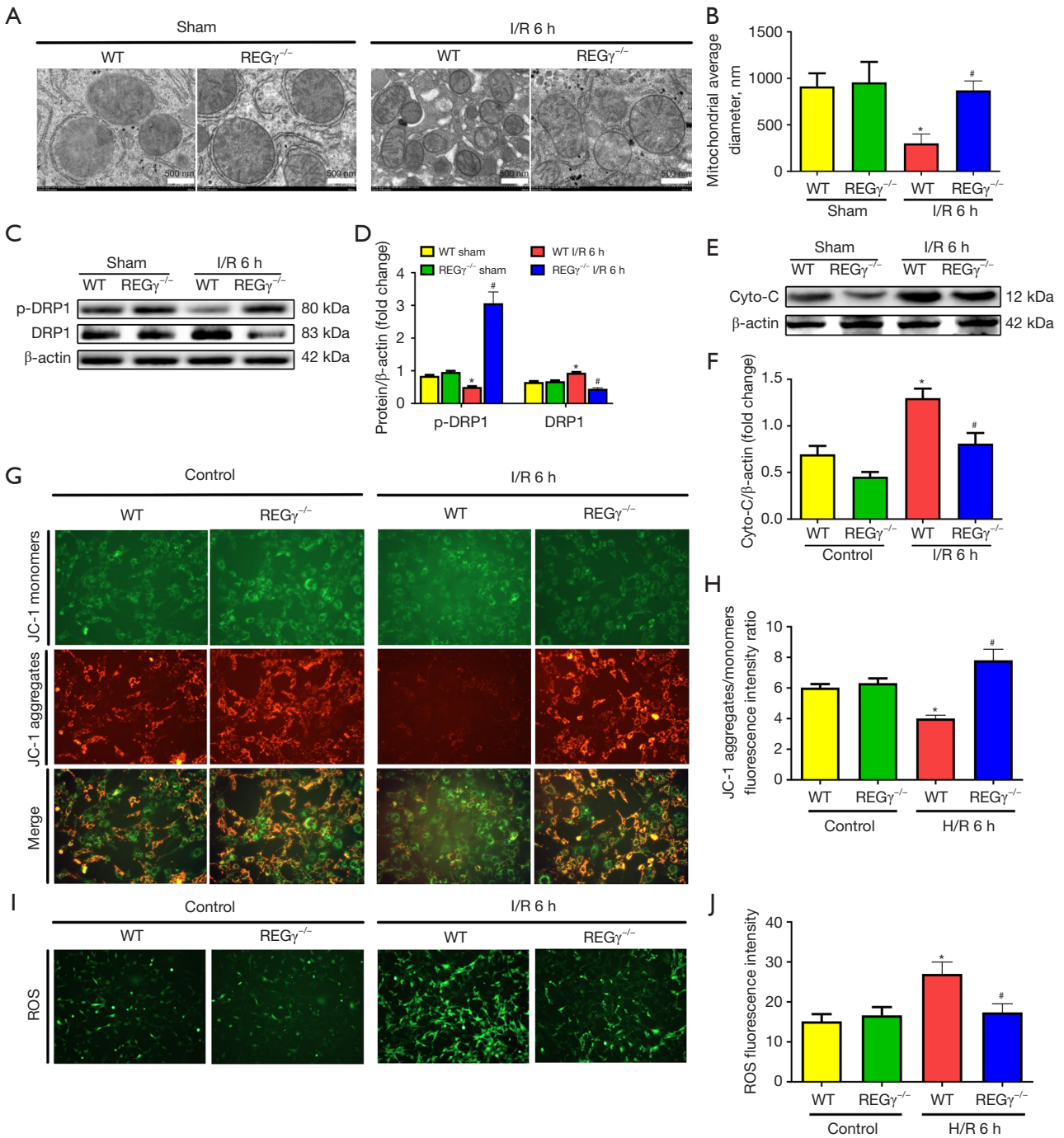

Figure 5 REGγ$^{-/-}$ inhibits hepatic mitochondrial injury in mice. *In vivo* experiment: Transmission electron microscopy, magnification 12,000×, scale bar 500 nm (A), Mitochondrial average diameter analysis (B); WB of p-DRP/DRP (C), gray value analysis (D); WB of Cytochrome C (E), gray value analysis (F); n=5 per group, *, P<0.05 *vs.* WT-Sham group; $^{\#}$, P<0.05 *vs.* WT-I/R group. *In vitro* experiments: JC-1 fluorescence staining 20× and MFI analysis (G,H). ROS fluorescence staining was performed 20×, and MFI analysis (I,J). n=5 per group, *, P<0.05 *vs.* WT-control group; $^{\#}$, P<0.05 *vs.* WT-H/R group. I/R, ischemia and reperfusion; WT, wild type; REG, the 11S proteasome regulatory complex; DRP, dynamin related protein 1; ROS, reactive oxygen species; WB, Western blot; MFI, mean fluorescence intensity; H/R, hypoxia and reoxygenation.

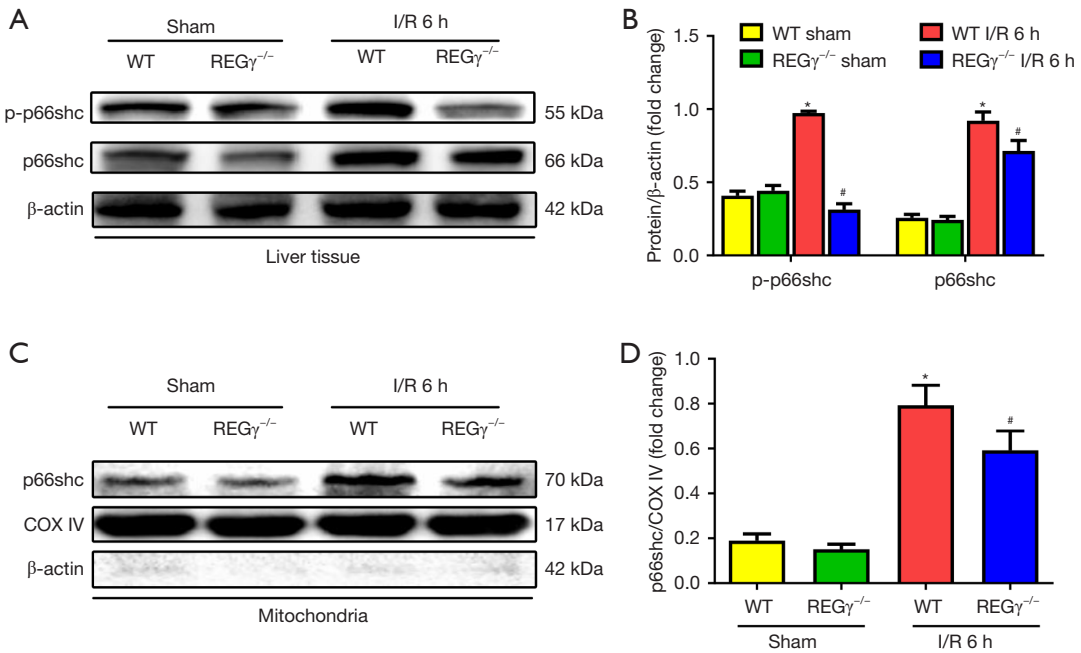

Figure 6 REGγ$^{-/-}$ reduces p66shc mitochondrial translocation in mice. WB of p-p66shc and p66shc in liver tissue (A), and gray value analysis (B); WB of mitochondrial p66shc in liver tissue (C), gray value analysis (D). n=5 per group, *, P<0.05 *vs.* WT-Sham group; $^{\#}$, P<0.05 *vs.* WT-I/R group. I/R, ischemia and reperfusion; WT, wild type; REG, the 11S proteasome regulatory complex; WB, Western blot.

the upregulation of autophagy. Therefore, REGγ represents a potential therapeutic target for lipid metabolism disorders. In contrast, the REGα and REGβ did not exert similar effects (18). REGγ expression was examined to investigate the role of REGγ in liver I/R injury. Our findings revealed that: during hepatic I/R injury, REGγ protein expression exhibited a marked increase while REGα and REGβ expressions remained unchanged.

Ischemic injury triggers aseptic immunoinflammatory response characterized by recruitment of Kupffer cells and neutrophils (24,25). The increased production of inflammatory factors further exacerbated hepatocyte death (26). Furthermore, the NF-κB signaling pathway plays a pivotal role in the progression of liver I/R injury, upon stimulation by I/R injury, NF-κB can be activated while IκB was inhibited and degraded, leading to the up-expression of proinflammatory mediators that contribute to hepatic damage (27). Therefore, we initially investigated the inflammatory response and found that REGγ KO significantly attenuated inflammatory cell infiltration, reduced pro-inflammatory cytokine release, and suppressed NF-κB signaling pathway phosphorylation levels.

In addition to inflammatory damage, apoptosis emerges as a crucial process associated with liver I/R injury (28,29). Therefore, we observed cellular apoptosis during liver I/R injury. The results demonstrated that REGγ KO mice exhibited significantly reduced levels of apoptosis. In conclusion, the deletion of the REGγ gene may exert a protective role in hepatic I/R injury by suppressing apoptosis.

Mitochondria are the most significant cellular organelles for adenosine triphosphate (ATP) generation, playing a vital role in regulating cellular redox, lipid metabolism, energy homeostasis and programmed cell death (30). The depletion of oxygen and nutrients during hepatic ischemia causes an extreme shortage of ATP in cells, which leads to the accumulation of ROS and acidic metabolites (31,32). Oxidative stress and calcium overload may promote the opening of mitochondrial transition pores with high permeability and the subsequent increase of mitochondrial membrane permeability. Additionally, cytochrome C, apoptotic proteins (such as BAX and caspase3) can be released from the intermembrane compartment (33), and eventually the cell becomes apoptotic or necrotic due to mitochondrial damage (34,35). Our findings demonstrate that REGγ KO leads to a significant reduction in the expression level of cytochrome C and significantly attenuated mitochondrial oxidative stress injury and

preserved mitochondrial membrane potential.

Dynamin related protein 1 (DRP1) plays a pivotal role in the division of mitochondrial. Upon phosphorylation at Ser637, DRP1 inhibits mitochondrial fission (36,37). In line with our electron microscopy findings, we observed a significant increase in the phosphorylation of DRP1 at Ser637 upon REGγ KO, suggesting that mitochondrial over division was inhibited by REGγ KO.

The bridging protein p66shc was encoded by the shc1 gene, is an important mitochondrial oxidoreductase (38,39). During the I/R process, the expression and phosphorylation levels of p66shc were up-regulated. Phosphorylated p66shc was further translated into mitochondria to oxidise cytochrome C and promote the production of ROS (40,41). However, whether REGγ contributes to mitochondrial oxidative stress damage by affecting p66shc phosphorylation levels and mitochondrial translocation is unclear. Our findings demonstrate that during hepatic I/R, REGγ KO mice exhibit reduced total protein and phosphorylation levels of p66shc as well as decreased mitochondrial translocation of this protein.

Based on the aforementioned experiments, we have confirmed that REGγ deficiency mitigates hepatic I/R injury in a mitochondrial p66shc dependent manner in mice. However, this study still has certain limitations and shortcomings. Firstly, further experiments are required to verify the signal molecules through which REGγ exerts its role in p66shc mitochondrial translocation. Secondly, my study did not explore the specific binding sites of each molecule, phosphorylation site, or block p66shc to validate the biological effect. Thirdly, the mechanism by which REGγ is transported from the nucleus to the cytoplasm and exerts its action remains unexplored.

Conclusions

Hepatic I/R injury remains a clinical challenge with limited effective intervention strategy. The findings of this study demonstrate that REGγ can modulate hepatic I/R injury, as evidenced by the significant reduction in liver injury, apoptosis, inflammatory response, and mitochondrial dysfunction observed upon REGγ KO. In addition, REGγ KO may exert an inhibitory effect on hepatic I/R injury through the regulation of mitochondrial p66shc-associated oxidative stress. These results contribute to a better understanding of the fundamental molecular mechanisms underlying hepatic I/R injury.

Acknowledgments

Funding: This study was funded by the National Natural Science Foundation of China (Nos. 82002016; 82272193).

Footnote

Reporting Checklist: The authors have completed the ARRIVE reporting checklist. Available at https://tgh.amegroups.com/article/view/10.21037/tgh-24-46/rc

Data Sharing Statement: Available at https://tgh.amegroups.com/article/view/10.21037/tgh-24-46/dss

Peer Review File: Available at https://tgh.amegroups.com/article/view/10.21037/tgh-24-46/prf

Conflicts of Interest: All authors have completed the ICMJE uniform disclosure form (available at https://tgh.amegroups.com/article/view/10.21037/tgh-24-46/coif). The authors have no conflicts of interest to declare.

Ethical Statement: The authors are accountable for all aspects of the work in ensuring that questions related to the accuracy or integrity of any part of the work are appropriately investigated and resolved. All experimental animals were approved by Clinical Center Laboratory Animal Welfare & Ethics Committee of Shanghai General Hospital, Shanghai Jiao Tong University (No. 2020AWS0032). All applicable international, national, and/or institutional guidelines for the care and use of animals were followed.

References

1. Al-Saeedi M, Steinebrunner N, Kudsi H, et al. Neutralization of CD95 ligand protects the liver against ischemia-reperfusion injury and prevents acute liver

failure. Cell Death Dis 2018;9:132.
2. Covington SM, Bauler LD, Toledo-Pereyra LH. Akt: A Therapeutic Target in Hepatic Ischemia-Reperfusion Injury. J Invest Surg 2017;30:47-55.
3. Hirao H, Nakamura K, Kupiec-Weglinski JW. Liver ischaemia-reperfusion injury: a new understanding of the role of innate immunity. Nat Rev Gastroenterol Hepatol 2022;19:239-56.
4. Rampes S, Ma D. Hepatic ischemia-reperfusion injury in liver transplant setting: mechanisms and protective strategies. J Biomed Res 2019;33:221-34.
5. Gudernatsch V, Stefańczyk SA, Mirakaj V. Novel Resolution Mediators of Severe Systemic Inflammation. Immunotargets Ther 2020;9:31-41.
6. Jiménez-Castro MB, Cornide-Petronio ME, Gracia-Sancho J, et al. Inflammasome-Mediated Inflammation in Liver Ischemia-Reperfusion Injury. Cells 2019;8:1131.
7. Guo L, Wu X, Zhang Y, et al. Protective effects of gastrin-releasing peptide receptor antagonist RC-3095 in an animal model of hepatic ischemia/reperfusion injury. Hepatol Res 2019;49:247-55.
8. Lecker SH, Goldberg AL, Mitch WE. Protein degradation by the ubiquitin-proteasome pathway in normal and disease states. J Am Soc Nephrol 2006;17:1807-19.
9. Whitby FG, Masters EI, Kramer L, et al. Structural basis for the activation of 20S proteasomes by 11S regulators. Nature 2000;408:115-20.
10. Mao I, Liu J, Li X, et al. REGgamma, a proteasome activator and beyond? Cell Mol Life Sci 2008;65:3971-80.
11. Harris JL, Alper PB, Li J, et al. Substrate specificity of the human proteasome. Chem Biol 2001;8:1131-41.
12. Li X, Lonard DM, Jung SY, et al. The SRC-3/AIB1 coactivator is degraded in a ubiquitin- and ATP-independent manner by the REGgamma proteasome. Cell 2006;124:381-92.
13. Li X, Amazit L, Long W, et al. Ubiquitin- and ATP-independent proteolytic turnover of p21 by the REGgamma-proteasome pathway. Mol Cell 2007;26:831-42.
14. Li L, Zhao D, Wei H, et al. REGγ deficiency promotes premature aging via the casein kinase 1 pathway. Proc Natl Acad Sci U S A 2013;110:11005-10.
15. Wang Q, Gao X, Yu T, et al. REGγ Controls Hippo Signaling and Reciprocal NF-κB-YAP Regulation to Promote Colon Cancer. Clin Cancer Res 2018;24:2015-25.
16. Lv Y, Meng B, Dong H, et al. Upregulation of GSK3β Contributes to Brain Disorders in Elderly REGγ-knockout Mice. Neuropsychopharmacology 2016;41:1340-9.
17. Lee FT, Mountain AJ, Kelly MP, et al. Enhanced efficacy of radioimmunotherapy with 90Y-CHX-A''-DTPA-hu3S193 by inhibition of epidermal growth factor receptor (EGFR) signaling with EGFR tyrosine kinase inhibitor AG1478. Clin Cancer Res 2005;11:7080s-6s.
18. Xu J, Zhou L, Ji L, et al. The REGγ-proteasome forms a regulatory circuit with IκBε and NFκB in experimental colitis. Nat Commun 2016;7:10761.
19. Matsushita M, Takasaki Y, Takeuchi K, et al. Autoimmune response to proteasome activator 28alpha in patients with connective tissue diseases. J Rheumatol 2004;31:252-9.
20. Yao L, Xuan Y, Zhang H, et al. Reciprocal REGγ-mTORC1 regulation promotes glycolytic metabolism in hepatocellular carcinoma. Oncogene 2021;40:677-92.
21. Yang L, Wang W, Wang X, et al. Creg in Hepatocytes Ameliorates Liver Ischemia/Reperfusion Injury in a TAK1-Dependent Manner in Mice. Hepatology 2019;69:294-313.
22. Gan J, Ji CF, Mao XR, et al. Synchronization isolation method for multiple types of cells from mouse liver. Zhonghua Gan Zang Bing Za Zhi 2023;31:532-7.
23. Alwadei N, Rashid M, Chandrashekar DV, et al. Generation and Characterization of CYP2E1-Overexpressing HepG2 Cells to Study the Role of CYP2E1 in Hepatic Hypoxia-Reoxygenation Injury. Int J Mol Sci 2023;24:8121.
24. Chen C, Wang Q, Yang Z, et al. Multiple machine learning methods and comparative transcriptomics identify pivotal genes for ischemia-reperfusion injury in human donor tissue undergoing orthotopic liver transplantation. Shock 2024;61:229-39.
25. Borjas T, Jacob A, Yen H, et al. Inhibition of the Interaction of TREM-1 and eCIRP Attenuates Inflammation and Improves Survival in Hepatic Ischemia/Reperfusion. Shock 2022;57:246-55.
26. Xu D, Qu X, Tian Y, et al. Macrophage Notch1 inhibits TAK1 function and RIPK3-mediated hepatocyte necroptosis through activation of β-catenin signaling in liver ischemia and reperfusion injury. Cell Commun Signal 2022;20:144.
27. Zhou H, Zhou S, Shi Y, et al. TGR5/Cathepsin E signaling regulates macrophage innate immune activation in liver ischemia and reperfusion injury. Am J Transplant 2021;21:1453-64.
28. Yao Z, Liu N, Lin H, Zhou Y. Proanthocyanidin Alleviates Liver Ischemia/Reperfusion Injury by Suppressing Autophagy and Apoptosis via the PPARα/PGC1α Signaling Pathway. J Clin Transl Hepatol

2023;11:1329-40.
29. Ye L, He S, Mao X, et al. Effect of Hepatic Macrophage Polarization and Apoptosis on Liver Ischemia and Reperfusion Injury During Liver Transplantation. Front Immunol 2020;11:1193.
30. Ma X, McKeen T, Zhang J, et al. Role and Mechanisms of Mitophagy in Liver Diseases. Cells 2020;9:837.
31. Machado IF, Palmeira CM, Rolo AP. Preservation of Mitochondrial Health in Liver Ischemia/Reperfusion Injury. Biomedicines 2023;11:948.
32. Park MN, Rahman MA, Rahman MH, et al. Potential Therapeutic Implication of Herbal Medicine in Mitochondria-Mediated Oxidative Stress-Related Liver Diseases. Antioxidants (Basel) 2022;11:2041.
33. Calis Z, Dasdelen D, Baltaci AK, Mogulkoc R. Naringenin Prevents Inflammation, Apoptosis, and DNA Damage in Potassium Oxonate-Induced Hyperuricemia in Rat Liver Tissue: Roles of Cytochrome C, NF-κB, Caspase-3, and 8-Hydroxydeoxyguanosine. Metab Syndr Relat Disord 2022;20:473-9.
34. Rao Z, Sun J, Pan X, et al. Hyperglycemia Aggravates Hepatic Ischemia and Reperfusion Injury by Inhibiting Liver-Resident Macrophage M2 Polarization via C/EBP Homologous Protein-Mediated Endoplasmic Reticulum Stress. Front Immunol 2017;8:1299.
35. Kantrow SP, Gierman JL, Jaligam VR, et al. Regulation of tumor necrosis factor cytotoxicity by calcineurin. FEBS Lett 2000;483:119-24.
36. Steffen J, Ngo J, Wang SP, et al. The mitochondrial fission protein Drp1 in liver is required to mitigate NASH and prevents the activation of the mitochondrial ISR. Mol Metab 2022;64:101566.
37. Chen Y, Yang C, Zou M, et al. Inhibiting mitochondrial inflammation through Drp1/HK1/NLRP3 pathway: A mechanism of alpinetin attenuated aging-associated cognitive impairment. Phytother Res 2023;37:2454-71.
38. Grandl G, Wolfrum C. Hemostasis, endothelial stress, inflammation, and the metabolic syndrome. Semin Immunopathol 2018;40:215-24.
39. Boengler K, Bornbaum J, Schlüter KD, et al. P66shc and its role in ischemic cardiovascular diseases. Basic Res Cardiol 2019;114:29.
40. Shan W, Gao L, Zeng W, et al. Activation of the SIRT1/p66shc antiapoptosis pathway via carnosic acid-induced inhibition of miR-34a protects rats against nonalcoholic fatty liver disease. Cell Death Dis 2015;6:e1833.
41. Vono R, Fuoco C, Testa S, et al. Activation of the Pro-Oxidant PKCβII-p66Shc Signaling Pathway Contributes to Pericyte Dysfunction in Skeletal Muscles of Patients With Diabetes With Critical Limb Ischemia. Diabetes 2016;65:3691-704.

doi: 10.21037/tgh-24-46
Cite this article as: Guo L, Yang Q, Zhu J, Li J. REGγ deficiency ameliorates hepatic ischemia and reperfusion injury in a mitochondrial p66shc dependent manner in mice. Transl Gastroenterol Hepatol 2024;9:62.